

META-TYROSINE CONJUGATES LABELED ⁶⁴CU AND ⁶⁸GA AS A CANCER RADIODIAGNOSIS AGENT USING MOLECULAR DOCKING SIMULATION ON LAT-1

HOLIS ABDUL HOLIK^{1,5*} , ANGELA ELYSIA ELAINE¹, BERNAP DWI PUTRA SITINJAK¹, FAISAL MAULANA IBRAHIM¹ , ARIFUDIN ACHMAD² , B. S. ARI SUDARMANTO³, HARYONO⁴ , ACHMAD HUSSEIN SUNDAWA KARTAMIHARDJA² 

¹Department of Pharmaceutical Analysis and Medicinal Chemistry, Faculty of Pharmacy, Universitas Padjadjaran, Sumedang-45363, West Java, Indonesia. ²Department of Nuclear Medicine, Faculty of Medicine/Universitas Padjadjaran, Sumedang-45363, West Java, Indonesia.

³Department of Pharmaceutical Chemistry, Faculty of Pharmacy, Universitas Gadjah Mada, Yogyakarta-55281, Yogyakarta, Indonesia.

⁴Department of Chemistry, Faculty of Life Sciences, Universitas Padjadjaran, Sumedang-45363, West Java, Indonesia. ⁵Research Collaboration Center for Theranostic Radiopharmaceuticals, Universitas Padjadjaran, Sumedang-45363, West Java, Indonesia

*Corresponding author: Holis Abdul Holik; *Email: holis@unpad.ac.id

Received: 17 Aug 2023, Revised and Accepted: 07 Oct 2023

ABSTRACT

Objective: This *in silico* study aims to determine the most potential compound of meta-tyrosine (JX-075, JX-078, and JX-119) ⁶⁴Cu and ⁶⁸Ga conjugated with various bifunctional chelating agents, NOTA, DOTA, and NODAGA, against the antiporter site of the LAT1 as conduct to develop a cancer diagnostic compound.

Methods: Molecular docking simulation was performed to investigate the interactions between meta-tyrosine compounds and LAT-1. Ligand compounds were drawn in 2D structures using ChemDraw Professional 16.0 and then labeled with ⁶⁴Cu and ⁶⁸Ga to build a radiopharmaceutical scaffold. The docking process was validated, characterized, and evaluated the interaction using several docking protocols in MOE 2020, a license owned by Gadjah Mada University. A visualization of the protein with the ligand was carried out on the BIOVIA Discovery Studio 2020.

Results: Docking simulation results show that JX119 has greater potential due to lower bond energy, JX119_NODAGA-⁶⁸Ga of -9.22 kcal/mol and JX119_NODAGA-⁶⁴Cu of -9.09 kcal/mol. This compound showed interactions with transporter amino acid sites Tyr259 and Phe252, both JX-119_NODAGA ⁶⁸Ga and JX119_NODAGA-⁶⁴Cu.

Conclusion: The compounds [⁶⁴Cu]Cu-NODAGA-JX119 and [⁶⁸Ga]Ga-NODAGA-JX119 are the most potential compounds with the lowest (most negative) Gibbs energy as conduct to develop a diagnostic compound.

Keywords: Cancer, Radiopharmaceuticals, LAT-1, Meta-tyrosine, Molecular docking

© 2023 The Authors. Published by Innovare Academic Sciences Pvt Ltd. This is an open access article under the CC BY license (<https://creativecommons.org/licenses/by/4.0/>) DOI: <https://dx.doi.org/10.22159/ijap.2023.v15s2.30> Journal homepage: <https://innovareacademics.in/journals/index.php/ijap>

INTRODUCTION

Cancer is the abnormal growth of cells that are not controlled, then attacks the body's physiological functions and can spread to other normal organs in the body. Cancer is the second leading cause of death in the world [1]. According to data reported by the Global Burden of Cancer (GLOBOCAN), in 2020, cancer cases in the world reached 19,292,789 new cases [2]. GLOBOCAN predictions for the next 20 to 30 y, the trend of cancer cases will continue to increase. This presents a challenge to develop an innovation that can improve the quality of life and the quality of treatment for cancer.

The best strategy to decrease cancer morbidity is early identification. Unfortunately, the methods used for cancer detection are currently ineffective, including overdiagnosis, inaccurate, less sensitive, and damage to normal tissues [3]. Thus, a renewable detection that can accurately assess the growth of cancerous or precancerous tissue is needed. The currently developing method in cancer detection is "molecular targeted therapy," which detects specific molecules expressed in cancer growth pathways [4]. Large Neutral Amino Acid Transporters type-1) LAT-1 can potentially be used as a diagnostic and therapeutic target due to its specific and overexpressing ability on cancer cells [5]. LAT-1 is a transporter protein that specifically plays a role in supplying growing tumor cells with essential amino acids and using amino acids as nutrients to build biomass and signaling molecules through activating pro-growth pathways [6].

Several LAT-1 inhibitors like BCH (2-amino-2-norbornene carboxylic acid) and JPH 203 had been developed. BCH has disadvantages because it is not specific for LAT-1, has poor affinity, and requires large doses for antitumor effects (>10 mmol), leading

to increased toxicity [7, 8]. A study by Yan *et al.* (2021) reported types of meta-tyrosine compounds JX-075, JX-078, and JX-119, and examination results on colon cancer cell lines (HT-29) showed that JPH203, as gold standard LAT-1 inhibitor, had an IC₅₀ of 0.06 μM while the meta-tyrosine compounds had an IC₅₀ that was not too much different (IC₅₀ 0.10-0.25 μM). These showed that the three compounds have an effective IC₅₀ to be used as LAT-1 inhibitors [9].

Based on these findings, meta-tyrosine seemed appealing as a carrier agent for radiopharmaceuticals to target LAT-1. Due to their lower concentrations and greater accuracy for diagnostic reasons, radiopharmaceuticals have additional benefits. Radiopharmaceuticals consist of a radionuclide (radioactive metal) and a carrier substance. Radiopharmaceuticals for diagnostic purposes must be able to emit positron or gamma rays since they have less destructive energy (0.3 keV/m), which is necessary for diagnostic purposes [10]. Gamma rays are more secure and, have powerful penetration strength (33-164 mm) and are interpreted by gamma cameras like SPECT (Single-Photon Emission Computed Tomography) and PET (Positron Emission Tomography) [11]. The imaging result could reveal details about the location and severity of the malignancy.

Radiopharmaceuticals conducted using the radioactive metals ⁶⁴Cu and ⁶⁸Ga, which generate gamma rays having energies of 511 KeV (43%) with half-lives of 12.7 h and 890 KeV (90%) 68 min, respectively. However, it is not possible to directly label these meta-tyrosine molecules with these metals. ⁶⁴Cu and ⁶⁸Ga need a bifunctional chelating agent (BFCA) to bind the metal into the chelator to form a stable complex and enhance its stability. Several chelators have been known to build suitable complexes with ⁶⁴Cu and ⁶⁸Ga and the complexes have been coupled with biological compounds to form targeting agents [12]. Based on this background,

research was conducted to develop a diagnostic compound with a carrier agent for meta-tyrosine compounds and to find the best chelator that can compile ^{64}Cu and ^{68}Ga metal and interact well with LAT-1 using the *in silico* method.

MATERIALS AND METHODS

Ligands and protein preparation

Ligands are derivative compounds of meta-tyrosine conjugated with DOTA (2,2',2'',2'''-(1,4,7,10-tetraazacyclododecane-1,4,7,10-tetrayl) tetraacetic acid), NOTA',2''(2,2'-(1,4,7-triazacyclononane-1,4,7-triyl)triacetic acid), and NODAGA (1,4,7-triazacyclononane,1-glutaric acid-4,7-acetic acid) chelator, then labeled with ^{64}Cu and ^{68}Ga to build a radiopharmaceutical scaffold. The complex was obtained by drawing 2D structures using the ChemDraw Professional 16.0 program licensed to Faculty of Pharmacy Universitas Padjadjaran, then saved in. cdx format. The result from 2D structures was converted into 3D by running the 2D structures on the Chem3D 16.0 program to minimize its energy, then saved in. mol2 format. The minimized ligands repeated with entered MOE's software by using the menu 'compute'. The next step is to save the ligand in. mdb format [13].

The LAT-1 receptor (PDB ID: 7DSQ) included with the native ligand was downloaded from the Protein Data Bank website (www.rcsb.org). The native ligand (3,5-diiodotyrosine) and all small molecules around were removed from the protein, then electronic and stericity parameters were corrected using the 'quick-prep' tool (located on the protein toolbar) in the MOE application 2020. The resulting LAT-1 protein was then stored in. mdb format and continued for method validation and molecular docking simulations [13].

Validation of docking poses

The docking pose was validated using several docking protocols in MOE 2020. The docking protocol with the best Root-Mean-Square

Deviation (RMSD) result was chosen to be applied in the molecular docking simulation of ligands. The results of the validation are marked with the RMSD value less than 2 Å [14].

Molecular docking simulation

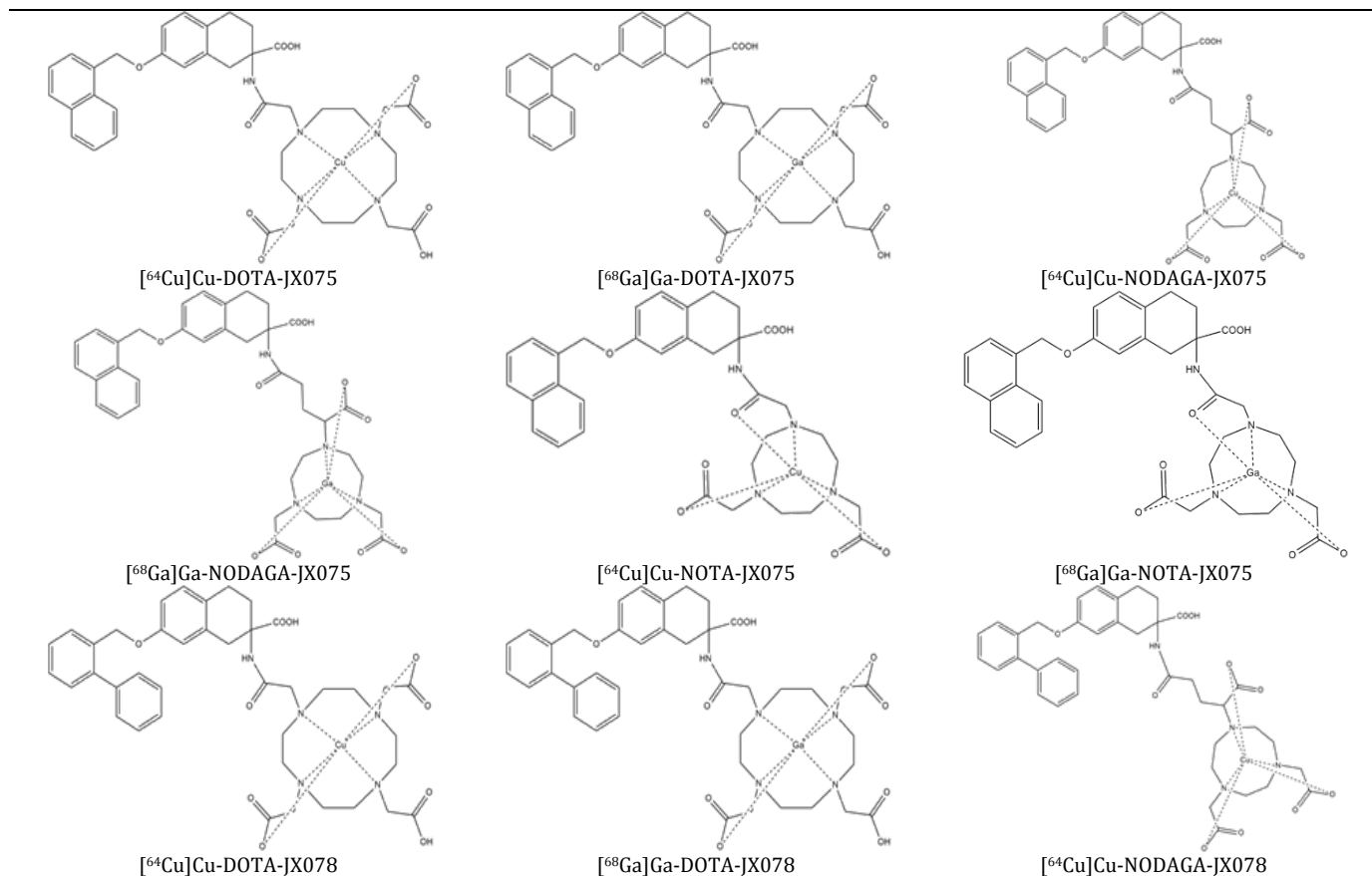
MOE software version 2020 was used in this study to help visualize, characterize, and evaluate the interaction of the protein with the test ligand. A database is created between ligands and JPH as comparison ligands using MOE 2020 for facilitating the molecular docking process. The database was saved in. mdb file format and continued running a procedure similar to the validation that was carried out. Then ΔG (Gibbs free energy) between the ligand and the receptor will be observed. Molecular docking simulation is accomplished by using the best docking protocol, specifically ligand atom (site), triangle matcher (placement), and induced fit (refinement). The top five docking poses out of 30 attempts were selected for data analysis. Each one of the ligands had docked, and their interactions had been observed. Aiming to observe hydrogen bonds between the ligand and the amino acid on the receptor, a visualization was carried out on the BIOVIA Discovery Studio application 2020 (<https://discover.3ds.com/discovery-studio-visualizer-download>). The visualization results are stored for later data analysis to determine whether ligands have the potential to be radio diagnostic for cancer [15].

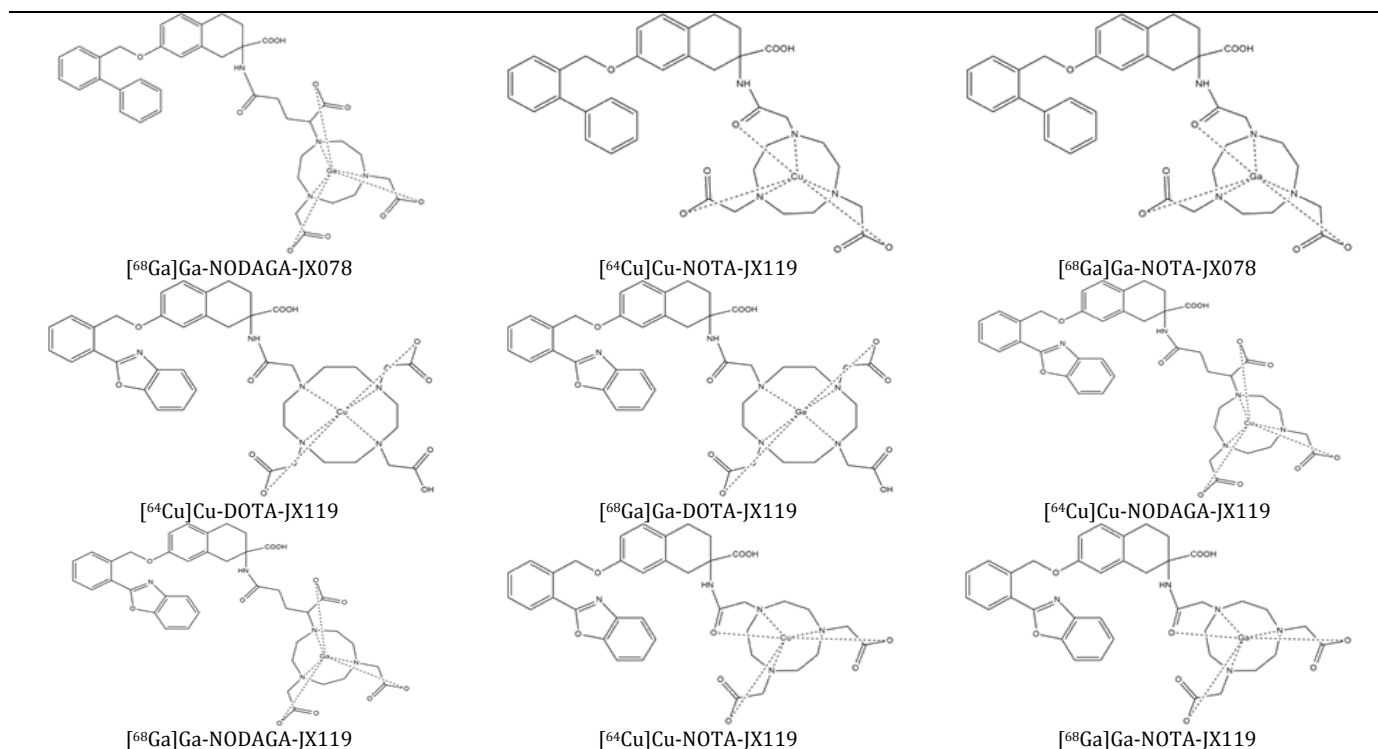
RESULTS

Radiopharmaceutical ligands preparation

The meta-tyrosine compound consisting of JX-075, JX-078, and JX-119 was conjugated with the NOTA and NODAGA chelators using the ChemDraw Professional 16.0 program which resulted in a 2-dimensional structure (table 1). An amide bond is formed between the primary amine group of the carrier compound and the carboxylic acid in the chelator.

Table 1: The 2D structure of radiopharmaceutical ligands





Validation of docking poses

The LAT-1 protein was prepared by protonating and correcting the amino acid sequence according to the sequence listed on

PDB. The LAT-1 protein and its native ligand (3,5-diiodotyrosine) were redocked using several molecular docking protocols to obtain the protocol with the best RMSD results (table 2).

Table 2: The docking protocol in the validation of docking poses process

Method	Site	WC	ph4	Placement	RMSD
General	Ligand	No	No	TM-IF	0.8212
General	Ligand	No	No	PMI-IF	0.5130
General	Ligand	Yes	No	TM-IF	0.8312
General	Ligand	Yes	No	PMI-IF	0.4806
General	Ligand	Yes	Yes	TM-IF	0.4858
General	Ligand	Yes	Yes	ph4-IF	0.4720
General	Pocket	Yes	No	PMI-IF	0.8941
General	Pocket	Yes	No	TM-IF	0.6546
General	Pocket	Yes	Yes	PMI-IF	0.4678
General	Pocket	Yes	Yes	TM-IF	0.4911
General	Pocket	Yes	Yes	ph4-IF	0.4720
TS	Ligan	Yes	No	IF	0.4731
TS	Pocket	Yes	No	IF	0.4737
TS	Pocket	Yes	Yes	IF	0.4784

The 3,5-diiodotyrosine pose of validation pose result from the redocking process was compared with the pose of 3,5-diiodotyrosine from PDB

(fig. 1). RMSD value of the redocking process is 0.4678 Å and fulfills the validation pose requirements RMSD value < 2.0 Å [14].

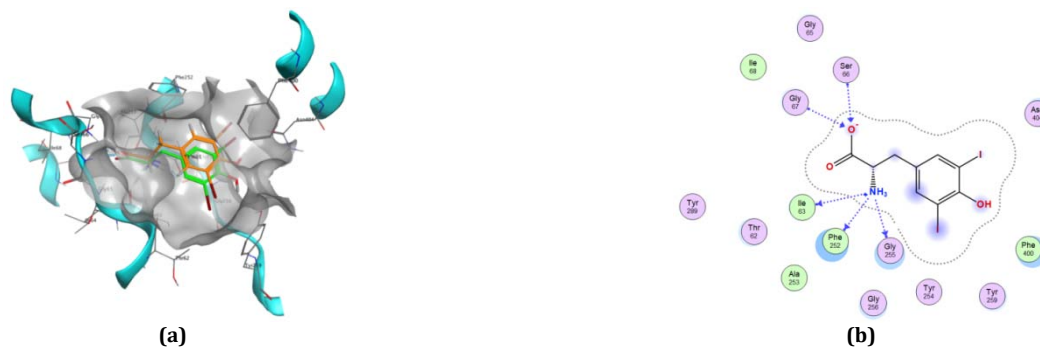


Fig. 1: Validation poses the result of LAT-1, (a) The 3,5-diiodotyrosine pose of the LAT-1 crystal structure (green) was compared with the 3,5-diiodotyrosine pose of the redocking result (orange), (b) Amino acid interaction of 3,5-diiodotyrosine and LAT-1

Docking result

Based on the molecular docking simulation process, Gibbs energy data was obtained, which illustrates the energy required for the interaction between the test ligand and LAT-1 protein as the target protein. The more negative the Gibbs energy value obtained, the interaction that occurs between the test ligand and the LAT-1 protein is more spontaneous and easier to occur [16]. In addition, interactions of amino acids in the LAT-1 protein with functional groups in the ligands were also obtained. The results of the molecular docking simulation can be seen in table 3.

Based on the conjugation with the active metal of the JX119 compound, the molecular docking simulation results show that JX119 has greater potential due to lower bond energy, $[^{68}\text{Ga}]\text{Ga-NODAGA-JX119}$ of -9.22 kcal/mol and $[^{64}\text{Cu}]\text{Cu-NODAGA-JX119}$ of -9.09 kcal/mol. When compared to the three chelators, both ^{64}Cu and ^{68}Ga metals, the compound with the NODAGA chelator showed the best potential with the lowest bond energy, while the compound with the NOTA chelator had the worst bond energy. Compounds $[^{68}\text{Ga}]\text{Ga-NODAGA-JX119}$ and $[^{64}\text{Cu}]\text{Cu-NODAGA-JX119}$ can bind to Tyr259 and Phe252 residues through Van Der Waals bonds (fig. 2).

Table 3: Molecular docking result

No	Ligand	Gibbs energy (kcal/mol)	Amino acid interaction	
			Hydrogen bond	Van der waals interaction
1	$[^{64}\text{Cu}]\text{Cu-DOTA-JX075}$	-7.39	Thr71	Phe400; Val148
2	$[^{68}\text{Ga}]\text{Ga-DOTA-JX075}$	-6.25	Ser66	Phe252*; Tyr259*
3	$[^{64}\text{Cu}]\text{Cu-NODAGA-JX075}$	-8.46	Ser66; Gly67; Gly65; Gly256	Phe252*; Gly255
4	$[^{68}\text{Ga}]\text{Ga-NODAGA-JX075}$	-8.10	Gly256; Ser66; Gly65	Phe252*
5	$[^{64}\text{Cu}]\text{Cu-NOTA-JX075}$	-3.50	-	-
6	$[^{68}\text{Ga}]\text{Ga-NOTA-JX075}$	-3.53	-	-
7	$[^{64}\text{Cu}]\text{Cu-DOTA-JX078}$	-7.14	Ser66; Gly256	Phe252*; Tyr259*; Phe400; Trp257*
8	$[^{68}\text{Ga}]\text{Ga-DOTA-JX078}$	-6.83	Val148	Phe400; Phe252*; Ser66
9	$[^{64}\text{Cu}]\text{Cu-NODAGA-JX078}$	-8.98	Gly256; Tyr71; Ser66	Phe252*; Gly255; Phe400; Tyr259*
10	$[^{68}\text{Ga}]\text{Ga-NODAGA-JX078}$	-7.97	Ser66; Gly65; Tyr259*	Phe400; Phe252*
11	$[^{64}\text{Cu}]\text{Cu-NOTA-JX078}$	-4.80	-	-
12	$[^{68}\text{Ga}]\text{Ga-NOTA-JX078}$	-4.58	-	-
13	$[^{64}\text{Cu}]\text{Cu-DOTA-JX119}$	-7.54	Asn404; Gly256; Ser66; Ser144	Val148; Phe252*; Tyr259*
14	$[^{68}\text{Ga}]\text{Ga-DOTA-JX119}$	-7.41	Ser66; Asn404; Gly256	Phe252*; Phe400; Tyr259*; Trp405
15	$[^{64}\text{Cu}]\text{Cu-NODAGA-JX119}$	-9.09	Thr71; Gly256; Asn404; Asn258	Tyr259*; Trp405; Val148; Phe400
16	$[^{68}\text{Ga}]\text{Ga-NODAGA-JX119}$	-9.22	Thr71; Ser66; Gly65; Asn404; Asn258	Phe252*; Tyr259*
17	$[^{64}\text{Cu}]\text{Cu-NOTA-JX119}$	-7.07	-	-
18	$[^{68}\text{Ga}]\text{Ga-NOTA-JX119}$	-6.54	-	-

*Amino acids on the LAT-1 antiporter site

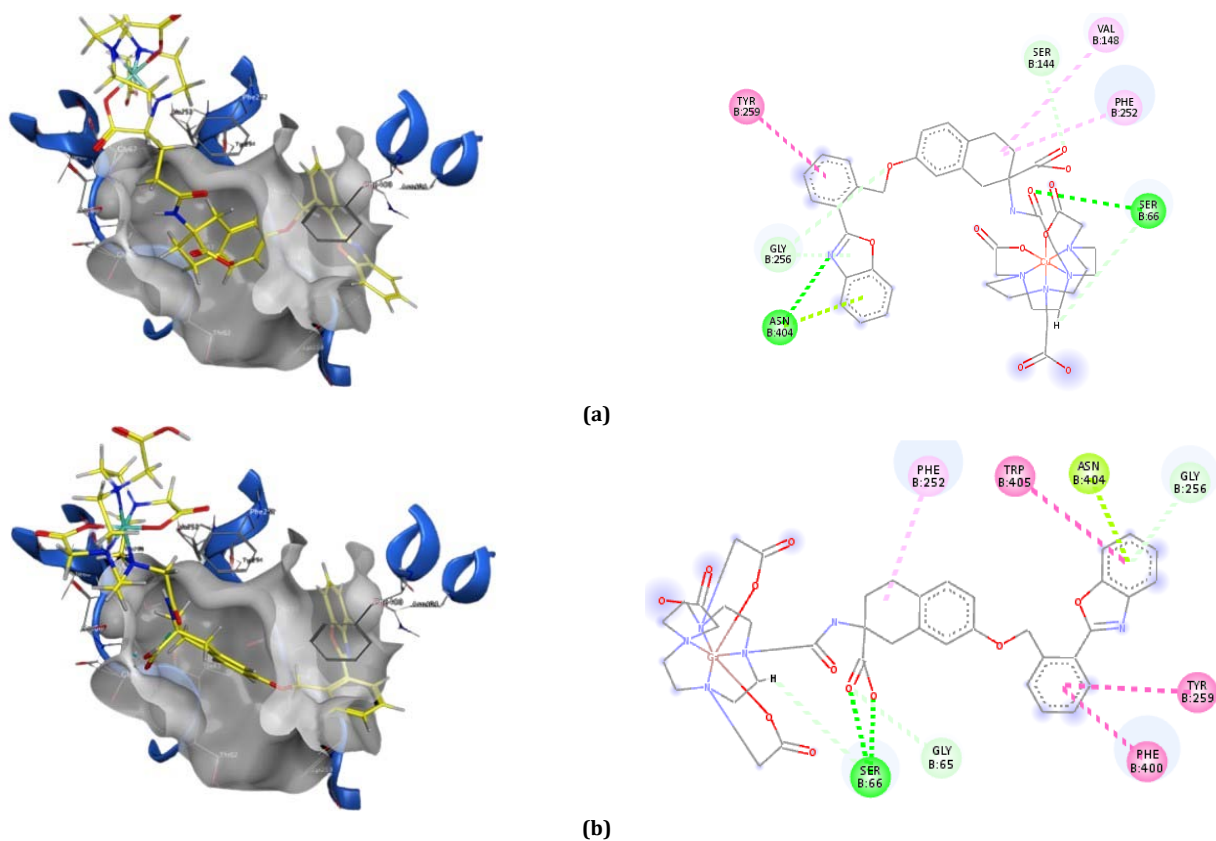


Fig. 2: (a) Visualization of interactions between $[^{64}\text{Cu}]\text{Cu-NODAGA-JX119}$ with LAT-1, (b) Visualization of interactions between $[^{68}\text{Ga}]\text{Ga-NODAGA-JX119}$ with LAT-1

DISCUSSION

The target molecule and the novel therapeutic compound may interact, and the molecular docking simulation technique will be able to discover and predict these interactions. Molecular docking simulation can aid in the more effective and efficient screening of many compounds during the research and development of new medicine.

JX-075, JX-078, and JX-119 are new compounds derived from bicyclic meta-tyrosine developed as LAT-1 inhibitors [9]. In the meta-tyrosine compound, the acidic part of JX will bind to the binding site in the unwound region of LAT-1 (TM1 and TM6), while the hydrophobic tail will bind to the TM10 region with detailed LAT-1 regions explained in Yan *et al.*, 2021 [8] and Singh *et al.*, 2018 [9]. This causes the prevention of the cycle of transport of amino acids into the cell. The JX inhibitor binds to LAT-1 in the same way as BCH

through the mechanism of the oxygen atom on the carboxyl and ammonium groups which form hydrogen bonds with the main chain atoms in the TM1 and TM6 regions. The interaction of JX compounds with LAT-1 can occur through the bonds of key amino acids such as Tyr289, Phe252, Val396 or Tyr117, Trp257, Asn258, Tyr259, and Arg348 [17].

The crystal structure of the protein target (fig. 3), LAT-1, was downloaded from the Protein Data Bank (PDB ID: 7DSQ) and prepared with MOE 2020 [13]. LAT-1 was prepared by removing all small molecules and water molecules around the protein molecule, except for the native ligand molecule, 3,5-diiodotyrosine [18]. Target proteins are also prepared by balancing polar hydrogens and protein charges to increase the susceptibility of the protein to the electronegative atoms of the ligands. Minimization of energy in the target protein is carried out to stabilize the protein so that molecular docking is achieved in a stable protein phase [19].

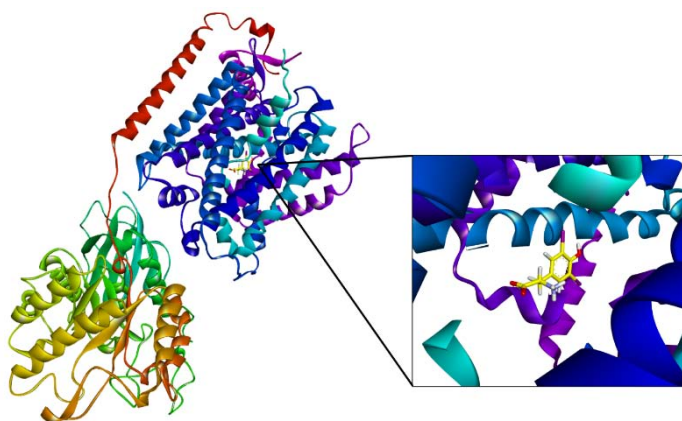


Fig. 3: The crystal structure of LAT-1 and native ligand 3,5-diiodotyrosine (yellow)

MOE software has been used in several studies to simulate the binding of ligand molecules to several biological targets. MOE is used in this study because it has an easy-to-use graphical interface. It represents a favorable graphical display of the results by showing the ligand and receptor binding residues with their positions and interactions [20]. Molecular docking simulation using MOE aims to find a favorable bond configuration between the ligand and the target protein. The process is carried out in a 3D docking box whose size depends on the selected atoms. The docking process begins with a random conformation of a predetermined conformation. In this study, the docking process was carried out using the conformation that had been determined at the pose validation step. The protocol that gives the lowest RMSD value in the pose validation stage is used for the molecular docking step [21].

In MOE, the receptor-ligand interaction affinities of all possible binding geometries are prioritized based on a numerical value called the *S*-score or it can be represented as a receptor-ligand binding energy value commonly interpreted as Gibbs energy [20]. Gibbs energy is obtained by calculating using the built-in potential function or grid-based potential field. The Gibbs energy calculated using the grid-based potential field method was calculated using electrostatic and van der Waals potential fields sampled on the grid lining the docking box. The grid-based method calculates the grid potential energy only at the start of the docking calculation [21, 22]. This method is faster than the built-in potential energy function.

Table 3 shows the results of the molecular docking simulation of the 18 test compounds. The JX119 compound conjugated with the NODAGA chelator has the most negative Gibbs free energy. Based on *in vitro* research by Yan *et al.* (2021), the JX078 compound is the compound with the smallest IC_{50} (121 nM) when compared to JX075 and JX119 with IC_{50} 165 nM and 234 nM respectively [9]. Because IC_{50} correlates with bond energy, the smaller the free energy of the Gibbs, the greater the potential of IC_{50} [23].

Chelators play a role in bond stability and influence pharmacokinetics. The NODAGA chelator is a derived macrocyclic

chelator used to chelate ^{64}Cu and ^{68}Ga . NODAGA can provide thermodynamic stability and has a suitable cavity size. ^{64}Cu has a tendency for high pharmacokinetic stability when conjugated to NODAGA. The NODAGA bond also forms a neutral bond with ^{68}Ga through conjugation with 3 carboxylates. Neutral conjugation causes lower hepatic uptake and better contrast against cancer cells [24].

CONCLUSION

Based on the results of molecular docking using MOE software, it was found that the compounds [^{64}Cu]Cu-NODAGA-JX119 ($S = -9.09$ kcal/mol) and [^{68}Ga]Ga-NODAGA-JX119 ($S = -9.22$ kcal/mol) are the compounds with the lowest (most negative) Gibbs energy. The more negative the Gibbs energy produced, the better and more spontaneous the interaction that can occur between the ligand compound and the target protein. Therefore, [^{68}Ga]Ga-NODAGA-JX119 and [^{64}Cu]Cu-NODAGA-JX119 are assumed to be able to interact better with LAT-1 protein when compared to other compounds. In addition, [^{68}Ga]Ga-NODAGA-JX119 interacts with three of the six key amino acids in the LAT-1 protein, namely the amino acids Phe252; Tyr259. Meanwhile, [^{64}Cu]Cu-NODAGA-JX119 interacts with two of the six key amino acids in the LAT-1 protein, namely the amino acids Phe252; Tyr259.

ACKNOWLEDGEMENT

This research was funded by the "Hibah Percepatan Lektor Kepala" grant from the Directorate of Research and Community Services Universitas Padjadjaran.

AUTHORS CONTRIBUTIONS

Conceptualization: HAH, FMI, AA; literature search and strategy: AA, FMI, AAE, BDP; data curation: HAH, AHSK, BSAS; writing-original draft preparation: FMI, AAE, BDP; visualization: AAE, BDP, BSAS; writing-review and editing: HAH, FMI, HY; project administration and funding acquisition: HAH, AA. All authors contributed to

revising and final drafting, agreed to the published version of the manuscript, and agreed to be responsible for every aspect of the job.

CONFLICT OF INTERESTS

All the authors declare no conflicts of interest.

REFERENCES

- Bray F, Laversanne M, Weiderpass E, Soerjomataram I. The ever-increasing importance of cancer as a leading cause of premature death worldwide. *Cancer*. 2021;127(16):3029-30.
- Sung H, Ferlay J, Siegel RL, Laversanne M, Soerjomataram I, Jemal A. Global cancer statistics 2020: GLOBOCAN estimates of incidence and mortality worldwide for 36 cancers in 185 countries. *CA Cancer J Clin*. 2021;71(3):209-49.
- Smith RA, Andrews KS, Brooks D, Fedewa SA, Manassaram Baptiste D, Saslow D. Cancer screening in the United States, 2019: a review of current American Cancer Society guidelines and current issues in cancer screening. *CA A Cancer J Clinicians*. 2019;69(3):184-210. doi: 10.3322/caac.21557.
- Yeong CH, Cheng M, Ng KH. Therapeutic radionuclides in nuclear medicine: current and future prospects. *J Zhejiang Univ Sci B*. 2014;15(10):845-63. doi: 10.1631/jzus.B1400131.
- Huttunen KM, Gynther M, Huttunen J, Puris E, Spicer JA, Denny WA. A selective and slowly reversible inhibitor of l-type amino acid transporter 1 (LAT1) potentiates antiproliferative drug efficacy in cancer cells. *J Med Chem*. 2016;59(12):5740-51. doi: 10.1021/acs.jmedchem.6b00190.
- Häfliger P, Charles RP. The L-type amino acid transporter LAT1-an emerging target in cancer. *Int J Mol Sci*. 2019;20(10):2428. doi: 10.3390/ijms20102428.
- Oda K, Hosoda N, Endo H, Saito K, Tsujihara K, Yamamura M. l-type amino acid transporter 1 inhibitors inhibit tumor cell growth. *Cancer Sci*. 2010;101(1):173-9. doi: 10.1111/j.1349-7006.2009.01386.x.
- Singh N, Ecker G. Insights into the structure, function, and ligand discovery of the large neutral amino acid transporter 1, LAT1. *Int J Mol Sci*. 2018;19(5):1278. doi: 10.3390/ijms19051278.
- Yan R, Li Y, Muller J, Zhang Y, Singer S, Xia L. Mechanism of substrate transport and inhibition of the human LAT1-4F2hc amino acid transporter. *Cell Discov*. 2021;7(1):16. doi: 10.1038/s41421-021-00247-4.
- Sgouros G, Bodei L, McDevitt MR, Nedrow JR. Radiopharmaceutical therapy in cancer: clinical advances and challenges. *Nat Rev Drug Discov*. 2020;19(9):589-608. doi: 10.1038/s41573-020-0073-9.
- Knapp FF, Dash A. *Radiopharmaceuticals for therapy*. Berlin: Springer India; 2016.
- Wadas TJ, Wong EH, Weisman GR, Anderson CJ. Coordinating radiometals of copper, gallium, indium, yttrium, and zirconium for PET and SPECT imaging of disease. *Chem Rev*. 2010;110(5):2858-902. doi: 10.1021/cr900325h.
- Alnajjar R, Mostafa A, Kandeil A, Al-Karmalawy AA. Molecular docking, molecular dynamics, and *in vitro* studies reveal the potential of angiotensin II receptor blockers to inhibit the COVID-19 main protease. *Heliyon*. 2020;6(12):e05641. doi: 10.1016/j.heliyon.2020.101612.
- Ramirez D, Caballero J. Is it reliable to take the molecular docking top-scoring position as the best solution without considering available structural data? *Molecules*. 2018;23(5):1038. doi: 10.3390/molecules23051038.
- Afriza D, Suriyah WH, Ichwan SJA. *In silico* analysis of molecular interactions between the anti-apoptotic protein survivin and dentatin, nordentatin, and quercetin. In: *Journal of physics*. Vol. 1073. IOP Publishing; 2018. p. 032001.
- Popovitz M. Formulas for death and life: chemical composition and biothermodynamic properties of monkeypox (MPV, MPXV, HMPXV) and vaccinia (VACV) viruses. *Therm Sci*. 2022;26:4855-68. doi: 10.2298/TSCI220524142P.
- Napolitano L, Galluccio M, Scalise M, Parravicini C, Palazzolo L, Eberini I. Novel insights into the transport mechanism of the human amino acid transporter LAT1 (SLC7A5). Probing critical residues for substrate translocation. *Biochim Biophys Acta (BBA) Gen Subj*. 2017;1861(4):727-36. doi: 10.1016/j.bbagen.2017.01.013.
- Pogorelov v T. Protein-ligand docking with MOE: introduction; 2011.
- Alghamdi HA, Attique SA, Yan W, Arooj A, Albulym O, Zhu D. Repurposing the inhibitors of COVID-19 key proteins through molecular docking approach. *Process Biochem*. 2021;110:216-22. doi: 10.1016/j.procbio.2021.08.015.
- Attique S, Hassan M, Usman M, Atif R, Mahboob S, Al-Ghanim K. A molecular docking approach to evaluate the pharmacological properties of natural and synthetic treatment candidates for use against hypertension. *Int J Environ Res Public Health*. 2019;16(6):923.
- Vilar S, Cozza G, Moro S. Medicinal chemistry and the molecular operating environment (MOE): application of QSAR and molecular docking to drug discovery. *Curr Top Med Chem*. 2008;8(18):1555-72.
- Ye WL, Shen C, Xiong GL, Ding JJ, Lu AP, Hou TJ. Improving docking-based virtual screening ability by integrating multiple energy auxiliary terms from molecular docking scoring. *J Chem Inf Model*. 2020;60(9):4216-30.
- Maffucci I, Contini A. Explicit ligand hydration shells improve the correlation between MM-PB/GBSA binding energies and experimental activities. *J Chem Theory Comput*. 2013;9(6):2706-17. doi: 10.1021/ct400045d.
- Satpati D, Sharma R, Sarma HD, Dash A. Comparative evaluation of ⁶⁸Ga-labeled NODAGA, DOTAGA, and HBED-CC-conjugated cNGR peptide chelates as tumor-targeted molecular imaging probes. *Chem Biol Drug Des*. 2018;91(3):781-8.